Chapter 3

Time-Domain Diffuse Optical Tomography for Breast Imaging: Background and Competing Imaging Modalities

Breast cancer has the highest incidence (30%) of all female cancer cases in the United States. About 10% of American women will develop breast cancer during their lifetime. An estimated 175,000 new cases will be diagnosed and 43,000 deaths will occur because of breast cancer each year. Even small improvements in the early diagnosis and treatment of breast cancer would likely save thousands of lives each year [1].

Cancer grows at an exponential rate with a doubling time of about three months. The preponderance of breast cancers are detected by patients themselves when the average size is about 2.5 cm. Unfortunately, about half of these have already metastasized to the lymph nodes. Breast cancer survival rates decrease form about 95% with a lesion size of 0.5 cm to only 75% or less when the cancer is treated at a size of about 2.5 cm [2].

An estimated 600,000 breast biopsies are performed each year in the United States based primarily on x-ray mammography and clinical breast examination (CBE) alone. Of these 85% were found to be benign [2]. The potential economic and quality of life benefits of improved diagnostic techniques would be substantial.

X-ray mammography and CBE are the current gold standards of breast cancer screening. Ultrasound and MRI are also used as secondary screening tools to elucidate

suspicious findings from the x-ray mammogram. Other non-optical imaging techniques include positron emission tomography (PET), electrical impedance tomography (EIT) and thermal imaging [3]. Recent advancements in x-ray mammography offer great promise including digital mammography and digital tomography. The alternatives to optical imaging are discussed in some detail in Section 3.1.

Ultimately the best approaches to breast cancer screening and diagnosis are likely to combine more than one imaging modality in co-registration. The acceptance of optical imaging as a clinical screening and/or diagnostic tool is likely to depend on the optical community coming to this realization. It is well established that optical imaging suffers from poor spatial resolution in comparison to other modalities such as x-ray and MRI imaging. Optical imaging, however, offers contrast to function of the breast, as opposed to structure, which may not be feasible with other modalities (in the absence of contrast agents). This is the basis of the multi-modality approach of the Time-Domain Optical Breast Imaging System described in this dissertation. This multi-modality approach combines the structural sensitivity of digital tomography with the functional sensitivity of time-domain optical tomography. Co-registration allows the x-ray data to be used as a constraint for improving the optical image and identifying boundaries. Ultimately, co-registration will permit fusion of x-ray and optical tomographic images through advanced image processing techniques. Research interest has also focused on combining MRI with optical imaging [4]. The combination with MRI is not proposed as a primary screening tool, but as a method of validating the efficacy of optical imaging.

The diffusion of light through a slab of tissue is discussed pictorially in Section 3.2. The three primary measurement schemes employed in optical imaging are discussed

along with the relative merits of each. Several clinical-level time-domain imaging systems are described from the literature to put perspective on the motivation for the design choices made relative to the Time-Domain Optical Breast Imaging System described in detail in Chapter 4.

3.1 Alternatives to Optical Imaging of the Breast

Alternatives to optical imaging of the breast are reviewed to provide insight into how optical techniques might improve on and/or compliment other imaging modalities. Most alternative imaging techniques provide only structural character of the breast tissue without the use of contrast agents. With the use of contrast agents, however, MRI and PET are both capable of providing functional information. Optical imaging is capable of assessing function either with or without contrast agents, is non-ionizing, relatively low cost and does not subject the patient to any radioactivity. Clearly, there is a likely role in the near future for optical imaging in the arsenal of imaging modalities that will prove important to early detection of cancerous lesions.

3.1.1 Film X-ray Mammography

X-ray mammography is based on the shadow left on film due to the absorption of low-energy x-ray photons by breast tissues. The breast is generally compressed between a polycarbonate compression plate on the cranial side and the film box on the caudal side. X-ray mammography, along with CBE, is the gold standard of breast cancer screening [1, 5]. The radiographic appearance of the female breast varies between individuals because of differences in the relative amounts of fat, connective and epithelial tissue, and because

of the different radiodensities of these tissues. Fat is radiographically lucent and appears dark on a mammogram, while connective and epithelial tissues are radiographically dense and appear light. The different radiological appearances created by variations in the relative amounts of these tissues are referred to as parenchymal patterns of the breast. These patterns can mask the underlying cancerous lesions, making interpretation of images difficult [6], particularly in the case of high-density breasts of young women.

A long-term follow-up study of the effects of radiation dose reports that the dose is suspected of inducing 0.2% of diagnosed cancers [7]. There is also the psychological factor to consider, which may decrease the willingness of a patient to undergo routine mammographic testing.

3.1.2 Digital Mammography

The film used in conventional x-ray mammography has a nonlinear response to x-ray photons. This results in limited dynamic range making it difficult to detect highly radiodense tissue from low radiodense tissue in the same exposure. The x-ray exposure must be very carefully set to prevent over or under exposure of the film. Digital x-ray, on the other hand has a very high dynamic range. This is a result of the wide dynamic response of the detectors commonly used, which are based on the combination of scintillating materials and silicon photodiode technology. Digital systems have the further advantage over film in that computers can be employed with sophisticated image processing capabilities to enhance contrast. The digital format also lends itself to the sharing of images over the Internet to allow for greater collaboration between radiologists and also allow for efficient data storage. One perceived disadvantage of digital imaging

is its lower spatial resolution relative to film. In practice, however, the effect of the lower spatial resolution is not observed relative to film, as the better spatial resolution of film is not realized due to its lower contrast. This has been demonstrated on the American College of Radiology (ACR) phantom for which no film systems presently in use can image all of the objects in the phantom in one exposure. The General Electric digital system can clearly image all objects in one exposure, despite having lower spatial resolution than film systems, due to its higher contrast resolution and dynamic range [5].

3.1.3 Digital Tomosynthesis

The major impediment to the detection of small cancers results from overlap with the normal tissues of the breast. The reduction in this "structure noise" is the primary advantage of tomography [5]. Conventional computed tomography (CT) would not work well because the patient's head and body would interfere with the required movement of the detector and x-ray tube. CT would also require significantly more dose. Tomography can, however, be achieved with the breast held in the standard mammography system and with a stationary detector. This is the basis of digital tomosythesis, which takes images obtained at low dose from a limited range of angles of the x-ray source and digitally shifts them so that only structures in the same plane align in the combined image. Structures in other planes are blurred due to misalignment, thereby enhancing the visibility of structures in the desired plane.

3.1.4 Ultrasound Tomography

Ultrasound uses high frequency reflected sound waves to produce an image of buried structures that have characteristically different densities. Ultrasound has evolved, not as a

replacement for x-ray mammography, but as a study best limited to the differentiation of cystic from solid lesions and as a guide for aspiration and biopsy [5].

One unusual characteristic of the breast is that relative to the parenchyma, fat in the breast is hypoechoic. This poses some problems for ultrasound because, with rare exceptions, breast cancers are hypoechoic [5]. A significant number of breast cancers are difficult if not impossible to see using ultrasound because they are isoechoic with fat or breast tissue.

3.1.5 Magnetic Resonance Imaging

Nuclear spin magnetic resonance imaging (MRI) without contrast enhancement has not proved very useful in the detection or diagnosis of breast cancer. Without contrast agents, MRI has failed to demonstrate sufficient sensitivity and specificity to justify the significant expense and time required [5]. Studies have suggested that contrast-enhanced scans may be helpful in determining the extent of breast cancer as a management aid, detecting unsuspected foci of multifocal or multicentric tumors and perhaps aiding in differentiation of benign from malignant lesions. MRI has also demonstrated efficacy in the evaluation of woman with silicone implants to demonstrate rupture of the implant. Pulse sequences that suppress signals from fat and water tissue make the differentiation of silicone possible.

The most likely clinical role of MRI is for the evaluation of women with known breast cancer, for which MRI will be used to assess the extent of the tumor and assist in treatment decisions. Contrast-enhanced MRI could have promise for the early detection of breast cancer as a screening tool, particularly in the radiographically dense breast, but only if the cost can be significantly reduced and the throughput increased.

3.1.6 Positron Emission Tomography

Positron emission tomography (PET) requires highly specialized and costly equipment. Reports have indicated that breast cancers have elevated metabolic activity that may be detected using fluorine 18-lableled glucose (FDG) to detect lesions that have an increased utilization of glucose [5]. This application for PET is limited by the requirement for the injection of radioactive material that is difficult to produce since it must be made using an on-site cyclotron due to its relatively short lifetime. PET scanning may be useful not only to determine whether a lesion is benign or malignant, but also to access some metabolic parameters that might be of prognostic value. PET has been reasonably successful at imaging large cancers, but has not been so successful at identifying cancers under 1 cm. Thus, while there seem to be some potential benefits of PET, its poor sensitivity to small lesions, requirement for subjecting the patient to radioactive substances, and high cost will likely preclude it from use as a primary screening tool [5,8].

3.1.7 Thermal Imaging

The basis of thermal mammography is the assumption that the angiogenisis associated with cancerous breast lesions causes increased flow and blood volume that can be detected by a high sensitivity thermal imager operating in the mid to long-wavelength range of the infrared spectrum. Typically, a comparison is made with the contralateral breast. Early attempts at this method were poorly received and have given the technology a bad reputation, as early versions of the thermal imagers were characterized by noise equivalent temperatures (NEΔT) of the order of 1 degree Celsius. State-of-the-art systems based on photovoltaic InSb focal plane arrays and GaAs quantum well

infrared photodetectors (QWIP) have improved NEΔT's to the order of 0.025 degrees Celsius. Renewed interest has developed in this technology since the advent of the high sensitivity cameras. Significant advantages of this technology are its relatively low system cost (the order of $100k) and lack of any ionizing radiation. The most significant disadvantage is that, due to the very high emissivity of tissue from water absorption, only thermal signatures on the surface of the skin can be detected. Thus, cancerous lesions near the surface may be readily detectable, but deep lying tumors would be substantially screened by the insulating properties of the breast tissues and by the diffusion of heat in reaching the surface. Thus, this technology may play a role in breast imaging, but could never be considered as a primary screening tool.

3.1.8 Electrical Impedance Tomography

Electrical impedance tomography (EIT) measures the distribution of impedance in a cross-section of the breast. This is possible because of the electrical resistivity variations of different breast tissues. By applying a series of small currents to the breast, a set of potential difference measurements can be made from non-current carrying pairs of electrodes. Since electric currents applied to the breast take the paths of least impedance, where the currents flow, depends on the subject's conductivity distribution [9].

EIT represents a potential, non-invasive technique to image women for breast cancer. Ex-vivo studies have shown characteristic frequency changes in the electrical conductivity (σ) and permittivity (ε) of cancerous versus normal tissue. By applying current around the periphery of the breast and measuring the resulting voltages, one can use computational model-based methods to reconstruct tomographic images of σ and ε inside the breast. This technology is in its infancy, but may represent a powerful new

modality in the arsenal of diagnostic mammographic techniques. It may also represent another modality that could be combined with optical imaging.

3.2 Optical Imaging Approaches

The three fundamental measurement schemes employed in imaging through diffusive media can be categorized as continuous wave (CW), frequency-domain (RF), and time-domain (TD) [10-14]. The important features and relative merits of each of the measurement schemes are described below.

The time-domain measurement scheme is generally believed to provide the most information about the nature of the diffuse photons and information regarding heterogeneities lying within the slab. The time-domain scheme represents the method used by the instrument described in detail in the next chapter. The various methods typically employed in the time-domain are discussed in order to understand their relative merits and to motivate the method used by the Time-Domain Optical Breast Imaging System described herein.

Figure 3.1 (A) illustrates how light diffuses through a slab of tissue. The signal photons enter on the left side of the slab. Multiple scattering causes the photons to spread out spatially as they progress through the slab. The effective width of the diffuse photons is greatest in the center of the slab, thus the poorest spatial resolution will occur for an object located midway between the source and detector. Symmetry rules result in the decrease of the effective width of the photons that are sensed in passing from the mid-plane of the tissue to the detector. Thus, the source and detector are interchangeable in the spatial sense. In the time-domain, the photons that arrive at the detector first will have traversed the shortest path and will therefore have the greatest spatial resolution.

For instance, the early arriving photons would be represented by the red path, intermediate arriving photons by orange, and late arriving photons by yellow in Figure 3.1 (A).

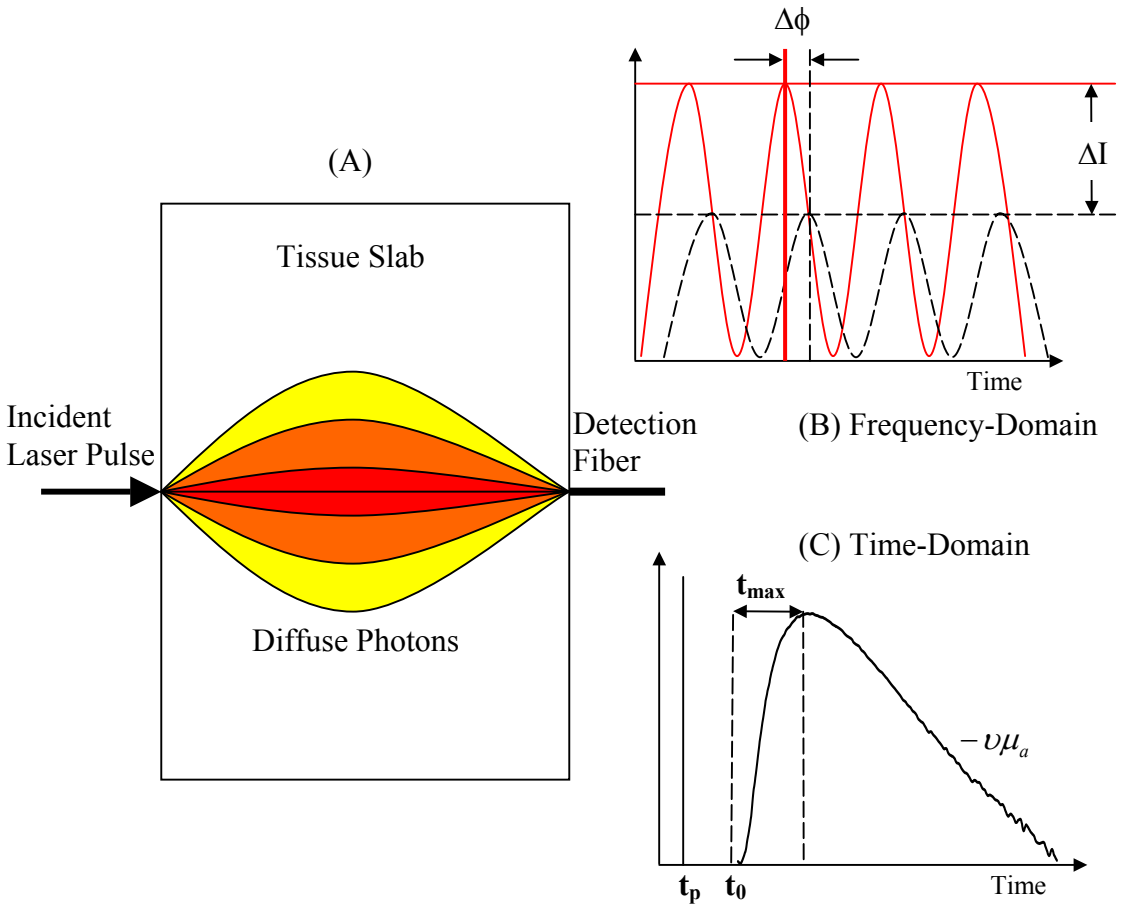

Figure 3.1 The diffusion of photons from a laser incident on the left side of a tissue slab is shown in (A). The photon paths form a "banana" pattern due to multiple scattering. In the frequency-domain, the phase of the RF-modulated source is shifted by an amount $\Delta\phi$ and the amplitude is attenuated by an amount ΔI at the detection fiber due to the delay and absorption induced by multiple scattering and absorption of the medium. The impulse response of photons traversing a diffuse slab is shown in (C) for the time-domain. The time to peak intensity of the temporal point spread function (TPSF) is indicated as t_{max}. The time of incidence of the pulse on the tissue is indicated as $\mathbf{t_p}$ and the time for the start of the TPSF by $\mathbf{t_0}$. The tail of the TPSF for long times falls of exponentially with a slope of $-\upsilon\mu_a$.

3.2.1 Continuous Wave

Continuous wave (CW) systems typically use a low modulation frequency LED or laser source incident on the tissue, either directly or through an optical fiber. The attenuated amplitude is measured directly by a photodetector or through an optical fiber interfaced to a photodetector. The use of multiple source-detector pairs allows for the reconstruction of 3-dimensional images and the use of multiple wavelengths permits spectroscopic imaging.

The purpose of modulating the source is to enable lock-in techniques to be used for improved noise performance and suppression of the effects of ambient background. This technique also permits multiple source wavelengths to be used simultaneously by modulation at different frequencies for different wavelengths, a process referred to as frequency-division multiplexing.

The consequence of measuring only the amplitude of the diffuse signal is that the absorption and scattering coefficients cannot be uniquely determined. This type of system, however, has the advantages of high signal-to-noise and relatively low cost. If the heterogeneities of interest primarily differ in the absorption coefficient, then very good images can be obtained by this method. For instance, if the major contrast is due to absorption of hemoglobin, lipids, or water, then this method can yield high sensitivity images of changes in the absorption coefficient $\Delta\mu_a$. In most breast tissues, however, there are likely to be changes in transmission due to changes in scattering coefficients, thus the CW measurements may not lead to accurate results, but they could very well lead to high contrast images. In the final analysis, high contrast to small changes in absorption or scattering may be all that is needed to identify a suspicious lesion.

3.2.2 Frequency-Domain

Frequency-domain (RF) systems generally use a single modulation frequency in the range of 70 MHz to 1 GHz in the radio frequency range. Beyond 1GHz the modulation depth is so small that the measurement is dominated by noise. The measurement scheme is depicted in Figure 3.1 (B). The effect of the absorption and scattering within the tissue is to delay the signal sensed at the detector by an amount $\Delta\phi$ and decrease its amplitude by an amount ΔI. Both the change in phase and amplitude are affected by the scattering and absorption coefficients, but the two independent measurements allow the scattering and absorption coefficients to be uniquely determined.

Theoretically, frequency-domain measurements made at multiple frequencies and time-domain measurements sampled at multiple times provide the same information, as they are Fourier Transforms of each other [4,10]. A frequency-domain system requires time to scan multiple frequencies and a time-domain system requires time to scan a number of time gates or to average enough signal to achieve acceptable performance. Generally, the initial phase ϕ_0 determination for frequency-domain systems is similar to the calibration issues of the initial time t_0 for the time-domain system. The complexities of RF circuitry, however, make it difficult to produce RF systems with multiple frequencies. Thus, most frequency-domain systems are single frequency and therefore generally have less information content relative to time-domain systems.

Typically, homodyne detection techniques are used to measure the in-phase and quadrature (IQ) demodulation components. Multiple wavelengths are accommodated by source modulation at slightly different frequencies, which again is a type of frequency-division multiplexing.

3.2.3 Time-Domain

The time-domain scheme is depicted in Figure 3.1 (C). The time of incidence of the delta function source pulse on the left side of the slab is indicated by $\mathbf{t_p}$. The time of the first photons to arrive at the detection fiber on the right side of the slab is indicated by $\mathbf{t_0}$. The time required for the first "ballistic" photons to arrive at the detection fiber is given by the ratio of the thickness of the slab and the speed of light in the medium. Ballistic photons travel in a nearly straight line between the source and detector, and undergo few, if any scattering events, thereby retaining their coherent properties. For a slab thickness relevant to breast imaging, the number of ballistic photons is so small as to be immeasurable. The earliest arriving photons are typically referred to as "snake" photons [14]. Snake photons have undergone a relatively small number of scattering events and undergo minimal spatial spreading in traversing between the source and detector. Therefore, they provide the highest spatial resolution that is measurable. The signal-to-noise of these snake photons is severely limited, however, for typical breast tissue thicknesses. They can provide useful spatial information for thin samples, but are not generally useful to breast imaging. Thus, the diffuse photons that constitute the bulk of the temporal point spread function (TPSF) are generally used in time-domain breast imaging. The time to the peak indicated by $\mathbf{t_{max}}$ is a function of both the absorption and scattering coefficient, but is generally dominated by the scattering coefficient. The slope of the exponential tail for long times, plotted as the natural log, is purely a function of the absorption coefficient and is equal to $-\mu_a \upsilon$, where υ is the speed of light in the medium. Thus, the absorption coefficient is available directly from the TPSF data, with no further processing or fitting required. The scattering coefficient can be determined by fitting the

TPSF to the diffusion model detailed in Chapter 2. The model must be convolved with the impulse response of the system to obtain accurate results.

Heterodyne, interferometric, and polarization techniques have been used to detect coherent photons in the time-domain. The thickness of breast tissue, however, results in essentially no detectable coherent photons, thus these techniques have no utility in breast imaging.

Incoherent time-domain measurement schemes include time-correlated single photon counting, streak camera, gated image-intensified CCD, optical Kerr gate, stimulated Raman amplification and second-harmonic cross-correlation [13]. The last three schemes were used early on, but have generally given way to the former three approaches.

Time-correlated single photon counting is regarded as the gold standard of time-domain measurement, representing the bulk of the time-domain systems in existence today. The time-delay of the photons incident on a high sensitivity quantum detector such as a photomultiplier tube (PMT) is measured with a time-to-amplitude converter. Even late arriving photons can be detected with a probability unbiased by the electronic detection scheme by keeping the probability of photon detection low [13]. A histogram of the arrival times is built up by averaging a large number of low energy pulses. Any system drift over the course of the averaging will result in drift in the amplitude of the TPSF, but will not alter its shape.

Streak cameras use a swept electric field to create an image on a CCD camera or image-intensified camera. The swept dimension of the image corresponds to the time axis. Thus, a complete TPSF can be imaged onto the CCD in a single frame. Multiple video frames can be averaged or the integration time can be increased to improve signal-

to-noise. The particular advantage to the use of a streak camera is its high temporal resolution that can be on the order of 1 psec [13]. Many investigators have opted to use the time-correlated approach over the streak camera due to the relatively higher system cost of the streak camera. Recent advances in image intensified CCD cameras, however, have caused a renewed interest in this measurement scheme.

The measurement scheme employed by the Time-Domain Optical Breast Imaging System is the gated, image-intensified CCD camera system (ICCD). The details of this system are described in Chapter 4. The basic approach uses a time-gated photocathode married to a high spatial resolution microchannel plate image-intensifier, the output of which is imaged onto a low noise, fast readout CCD camera. The gate is open for a short time relative to the width of the TPSF. By varying the delay time of the gate, a series of images represent time slices of the TPSF. A complete TPSF is built up of a finite number of discrete time gates. Signal-to-noise can be improved by increasing the number of averaged frames or increasing the integration time of the CCD camera. Any drift during the course of acquiring all the images that make up a single TPSF will result in an error in the shape of the TPSF, which is a disadvantage of this approach relative to time-correlated techniques. The very significant advantage of this approach is its potential for massively parallel detection afforded by the high resolution of the image intensifier and CCD. This is evidenced by the 313 detection fibers of the Time-Domain Optical Breast Imaging System. Thus, a much larger data set can be acquired in a limited amount of time, resulting in the potential for higher contrast-to-noise performance and higher spatial resolution in comparison with any other technique. Note that the streak camera approach

can only image detection fibers in one dimension, as the second dimension is taken up by the time scan.

3.3 Review of Past Work and Instrumentation in Time-Domain DOT Breast Imaging

The development of fully clinical-ready time-domain optical breast imaging systems is in its infancy relative to both CW and RF clinical mammographic systems. A search through the literature revealed six clinical-level time-domain imaging systems with application to breast imaging [15-23]. Five of the systems used the gold standard time-correlated approach. The other system used a streak camera. The features of these six systems are reviewed below. Also described below are two papers that illustrate the use of gated image intensified cameras similar to the system used by the Time-Domain Optical Breast Imaging System described in detail in Chapter 4.

Grosenick *et al.* describe a time-correlated single photon counting mammographic system utilizing a single source-detector fiber pair scanned in tandem at a single wavelength of 785 nm [15,16]. They report measuring 1500 scan positions with a 2.5 mm spacing within a time period of about 5 minutes. The 785 nm laser diode source had a pulse width of 400 ps with an average power of 5 mW at a maximum repetition rate of 80 MHz. The breast was compressed between two 6 mm thick glass plates. They describe broadening resulting from reflections from the surfaces of the compression plates, but make no mention of anti-reflection coatings and admit that the effects were not taken into account in their model. Strong edge effects were described along with correction algorithms for addressing the distortion of the TPSF at and near the boundaries. Their preliminary clinical results are very encouraging, readily resolving a

large tumor mass and even large veins, likely caused by congestive heart failure. They also describe a method of achieving limited depth resolution by shifting the relative position of the source and detection fibers. In its reported embodiment, the system has the disadvantage of operation at only one wavelength, ruling out any spectroscopic imaging capability. It has the further disadvantage of extremely limited depth resolution due to the use of a single source-detector pair. If this general approach was extended to multiple wavelengths and multiple detector positions for each source position, the measurement time would be unacceptably long for clinical use.

Cubeddu *et al.* describe a clinical time-correlated single photon counting mammographic imaging system that operated at four wavelengths simultaneously with the breast lightly compressed between two polycarbonate compression plates [18]. The four pulsed laser diodes emitted at wavelengths of 671, 795, 912, and 973 nm with an average output power of 4 mW at a repetition rate of 40 MHz, enabling sensitivity to hemoglobin, lipids, and water. Two different types of compact PMT's were used to cover the spectral range. The lower two wavelengths used a Hamamatsu model R5900-01-L16 PMT with spectral sensitivity up to 850 nm, while the longer two wavelengths used a Hamamatsu model H7422P-60 with extended near infrared response out to 1100 nm. They reported a measurement time of 5 minutes with a distance of 1 mm between measurement points for a continuous scan. They show early time gate images that clearly resolve a fibroadenoma from surrounding tissue with the greatest contrast for 912 nm, indicating low lipid content for the lesion relative to surrounding tissue. Again, this system is limited to 2-dimensional images due to the use of a single source-detector pair.

Ntziachristos *et al.* describe a time-correlated single photon counting mammographic imager employing 2 wavelengths, time-multiplexed into 24 source fibers, received in transmission mode between compression plates by 8 detection fiber bundles [4]. The system was designed to be used in concert with MRI for validating the optical imaging with an accepted imaging modality standard. The low-power laser diodes operated at 780 and 830 nm with an average power of 20 μW at a pulse repetition rate of 5 MHz. The 1 x 24 source optical switch was a mechanical type that is inherently slow, resulting in longer than necessary measurement times. Large 5 mm diameter detection fiber bundles were required due to the very low average powers of the laser diodes. Spatial resolution of the system was poor due to the small number of detection fibers. The time required for a complete scan was not described, but there was no particular time limit, given the relatively long period required for MRI imaging. Phantom results were very encouraging, providing good contrast for both absorption and scattering heterogeneities with minimal cross talk. Presumably, the system could be readily extended to more detectors with no impact on measurement time. The total measurement time, however, is likely to be much too long for routine clinical imaging. This could be corrected by use of a fast switching scheme such as is employed in the Time-Domain Optical Breast Imaging System describe in Chapter 4.

Perhaps the most widely documented time-correlated single photon counting system is that described by Schmidt *et al.* that makes use of 32 channels of coaxial source-detector pairs with a tunable Ti:Sapphire laser source [19-21]. The system is referred to as the multi-channel opto-electronic near-infrared system for time-resolved image reconstruction (MONSTIR). A set of 32 computer-controlled variable optical attenuators

is described that ensures that the intensity of light detected by nearby source-detector pairs does not saturate or damage the detectors. The system can be configured to operate in either reflectance or transmission modes. The detectors are comprised of a set of four 8-anode multichannel plate photomultiplier tubes, and incorporate long pass blocking filters to minimize the effects of ambient light. The system was designed to be rugged and portable and is housed in two large wheeled carts. The application was for premature and full term infants, but it could easily be applied to breast measurement as mentioned in the literature. A dedicated image reconstruction software package was used, known as TOAST (temporal optical absorption and scattering tomography) developed at University College London.

The MONSTIR system also lacks an efficient means for switching between source fibers, requiring a full 3.5 sec. This is 10,000 times slower than the novel fiber source multiplexing system described in detail in Chapter 4 as part of the Time-Domain Optical Breast Imaging System. If this system were required to make a breast measurement within a 2-minute period, almost the entire allotment of time would be taken up by switching between source fibers. Thus, perhaps it is not really that well suited for clinical breast measurement.

A very similar system to that of MONSTIR is described by Eda *et al.* for which the number of channels has been increased to 64 and the source replaced with laser diodes [21,22]. Three laser diodes were used with wavelengths of 761, 791, and 830 nm with a pulse width of 100 psec, 0.25 mW average power, and a modulation frequency of 5 MHz. The time required to measure an 8 cm diameter phantom was stated as 30 min. This long measurement time is a result of the low average power of the laser diode sources and the

slow fiber source switching time. The algebraic reconstruction technique was used as an inversion algorithm. This system is even less suitable than MONSTIR to breast imaging in clinically acceptable measurement times.

The last complete time-domain mammography system reviewed uses a streak camera as the detector. The system of Painchaud *et al.* used a Ti:Sapphire laser source at a pulse repetition frequency of 80 MHz [23]. The system represented an improvement on the standard single source-detector fiber pair scanning by incorporation of multiple detection fibers. The actual number of detection fibers scanned in parallel was not reported, but the group did report the acquisition of 15,000 locations in 7 minutes. The patient was supine positioned with the breast slightly compressed between two acrylic compression plates. The *in vivo* scans were reported to be capable of resolving blood vessels. This system should be capable of depth resolution, although no particular mention of this was made.

Valentini *et al.* reported in 2001 on the use of a fast, gated image-intensified CCD camera for time-domain optical imaging. The experimental set up used a mode-locked Argon laser emitting an average of 6 mW at 514 nm and the Picostar gated ICCD manufactured by LaVision of Goettingen, Germany. This report is interesting in that it uses the identical camera and in a similar fashion as that of the system described in this dissertation. Phantom measurements were made with the laser incident on one side of a tank filled with an aqueous solution of intralipid and India ink to simulate the optical properties typical of tissue.

Another optical imaging system using an ICCD is reported by Thompson *et al.* for near infrared fluorescence contrast-enhanced imaging [25]. Instead of using the gate to

acquire data in the time-domain, it was modulated in a homodyne frequency-domain scheme. It is described in the context of optical mammographic imaging.

3.4 Summary

Alternatives to optical breast imaging were described along with their benefits and disadvantages. The optimal application for optical breast imaging was described as a multi-modality imaging system in combination with the current gold standard, x-ray mammography. The three primary optical imaging schemes that include CW, frequency-domain, and time-domain imaging were described and compared. Time-domain measurements are generally regarded as having the richest information content. Several optical mammography-capable clinical imaging systems were discussed. Most systems either take too long for image acquisition or provide only 2-dimensional imaging, relative to that of the Time-Domain Optical Breast Imaging System described in Chapter 4.

Chapter 3 References

1. S. H. Landis, T. Murray, S. Bolden, and P. A. Wingo, "Cancer Statistics 1999", Cancer J. Clin. **49**, 8-31 (1999).
2. S. B. Colak, M. B. van der Mark, G. W. 't Hooft, J. H. Hoogenraad, E. S. van der Linden, and F. A. Kuijpers, "Clinical Optical Tomography and NIR Spectroscopy for Breast Cancer Detection," IEEE Journal of Selected Topics in Quantum Electronics **5,** 1143-1158 (1999).
3. D. A. Benaron and D. K. Stevenson, "Optical time-of-flight and absorbance imaging of biologic media," Science **259**, 1463-1466 (1993).
4. V. Ntziachristos, X. Ma, and B. Chance, "Time-correlated single photon counting imager for simultaneous magnetic resonance and near-infrared mammography," Rev. Sci. Instr. **69**, 4221-4233 (1998).
5. D. B. Kopans, Breast Imaging, Lippincott-Raven Publishers, Philadelphia, NY, 2nd Edition, 1998.
6. N. F. Boyd, G. A. Lockwood, J. Byng, D. L. Tritchler, and M. Yaffe, "Mammographic densities and breast cancer risk," Cancer Epidemiology, Biomarkers & Prevention (June 1998).
7. S. Chacko and M. Singh, "Three-dimensional reconstruction of transillumination tomographic images of human breast phantoms by red and infrared lasers," IEEE Transactions on Biomedical Engineering, **47**, 131-135 (2000).
8. A. E. Cerussi, A. J. Berger, F. Bevilacqua, N. Shah, D. Jakubowski, J. Butler, R. F. Holcombe, and B. J. Tromberg, "Sources of absorption and scattering contrast for near-infrared optical mammography," Acad. Rad. **8**, 211-218 (2001).
9. S. Meeson, "An investigation of optimal performance criteria in Electrical Impedance Tomography," PhD Thesis, University of Southampton, 1997.
10. J. J. Stott and D. A. Boas, "A practical comparison between time-domain and frequency-domain diffusive optical imaging systems," OSA Biomedical Topical Meetings, Advances in Optical Imaging and Photon Migration, 626-628 (2002).
11. F. Gao, H. Zhao, and Y. Yamada, "Improvement of image quality in diffuse optical tomography by use of full time-resolved data," Applied Optics **41**, 778-790 (2002).
12. V. Ntziachristos, A.G. Yodh, and Britton Chance, "Accuracy limits in the determination of absolute optical properties using time-resolved NIR spectroscopy," SPIE Optical Tomography and Spectroscopy of Tissue III **3597**, 213-220 (1999).
13. R. Berg, S. Andersson-Engles, and S. Svanberg, "Time-resolved transillumination imaging," Medical Optical Tomography: Functional Imaging and Monitoring **IS11**, 397-424 (1993).
14. K. M. Yoo, B. B. Das, F. Liu, and R. R. Alfano, "Ultrashort laser pulse propagation and imaging in biological tissue and model random media – steps towards optical mammography," Medical Optical Tomography: Functional Imaging and Monitoring **IS11**, 397-424 (1993).
15. D. Grosenick, H. Wabnitz, H. H. Rinneberg, K. T. Moesta, and P. M. Schlag, "Development of a time-domain optical mammogaph and first *in vivo* applications," Applied Optics **38**, 2927-2943 (1999).

16. D. Grosenick, H. Wabnitz, R. Macdonald, H. Rinneberg, J. Mucke, C. Stroszczynski, and P. Schlag, "Determination of *in vivo* optical properties of breast tissue and tumors using a laser pulse mammography," OSA Biomedical Topical Meetings, Advances in Optical Imaging and Photon Migration, 459-461 (2002).
17. R. Cubeddu, G. M. Danesini, E. Giambattistelli, F. Messina, L. Palloro, A. Pifferi, P. Taoni, and A. Torricelli, "Time-resolved optical mammography for clinical studies beyond 900 nm," OSA Biomedical Topical Meetings, Advances in Optical Imaging and Photon Migration, 674-676 (2002).
18. F. E. W. Schmidt, M. E. Fry, E. M. C. Hillman, J. C. Hebden, and D. T. Delpy, "A 32-channel time-resolved instrument for medical optical tomography," Rev. Sci. Instr. **71**, 256-265 (2000).
19. J. C. Hebden, F. M. Gonzalez, A. Gibson, E. M. C. Hillman, R. Md. Yusof, N. Everdell, D. T. Delpy, G. Zaccanti, and F. Martelli, "Assessment of an *in situ* temporal calibration method for time-resolved optical tomography," Journal of Bio. Opt. **8**, 87-92 (2003).
20. J. C. Hebden, T. Bland, E. M. C. Hillman, A. Gibson, N. Everdell, D. T. Delpy, S. R. Arridge, and M. Douek, "Optical tomography of the breast using a 32-channel time-resolved imager," OSA Biomedical Topical Meetings, Advances in Optical Imaging and Photon Migration, 187-189 (2002).
21. H. Eda, I. Oda, Y. Ito, Y. Wada, Y. Tsunazawa, M. Takada, Y. Tsuchiay, Y. Yamashita, M. Oda, A. Sassaroli, Y. Yamada, and M. Tamura, "Multichannel time-resolved optical tomographic imaging system," Rev. Sci. Instr. **70**, 3595-3602 (1999).
22. F. Gao, H. Zhao, Y. Onodera, A. Sassaroli, Y. Tanikawa, and Y. Yamada, "Image reconstruction from experimental measurements of an multichannel time-resolved optical tomographic imaging system," SPIE Optical Tomography and Spectroscopy of Tissue IV **4250**, 351-361 (2001).
23. Y. Painchaud, A. Mailloux, E. Harvey, S. Verreault, J. Frechette, C. Gilbert, M. L. Vernon, and P. Beaudry, "Multi-port time-domain laser mammography: results on solid phantom and volunteers," SPIE Optical Tomography and Spectroscopy of Tissue III **3597**, 548-555 (1999).
24. G. Valentini, C. D'Andrea, D. Comelli, and R. Cubeddu, "Use of a fast gated CCD camera for imaging through turbid media," SPIE Optical Tomography and Spectroscopy of Tissue IV **4250**, 191-195 (2001).
25. A. B. Thompson and E. M. Sevick-Muraca, "Near-infrared fluorescence contrast-enhanced imaging with intensified charge-coupled device homodyne detection: measurement precision and accuracy," J. Bio. Opt. **8**, 111-120 (2003).